Phonon dispersion relations for potassium thiocyanate at and above room temperature

1992 J. Phys.: Condens. Matter 4 7851

(http://iopscience.iop.org/0953-8984/4/39/001)

J. Phys.: Condens. Matter 4 (1992) 7851–7864. Printed in the UK

Phonon dispersion relations for potassium thiocyanate at and above room temperature

D J Cookson†, M M Elcombe‡ and T R Finlayson†

† Department of Physics, Monash University, Clayton, Victoria 3168, Australia
‡ Australian Nuclear Science and Technology Organisation, Lucas Heights Laboratories, Lock Mailbag, Menai, New South Wales 2234, Australia

Received 6 May 1992

Abstract. The elastic stiffness constants of KSCN have been measured using a pulse-echo-overlap method at 10 MHz and compared to those for CsSCN. In both crystals it was found that transverse waves propagating normal to the mirror planes encountered the greatest shear stiffness. Room temperature inelastic neutron scattering has been used to measure phonon energies of less than 5 THz in KSCN at various positions in reciprocal space. At higher temperatures the acoustic phonon resonances were found to soften gradually, while the optic modes exhibited largely unpredictable changes in width, frequency and intensity.

1. Introduction

Potassium thiocyanate (KSCN) has been the most widely studied of all the thiocyanates. The room-temperature crystal structure (figure 1) was first determined by Klug in 1933 [1] from single-crystal, x-ray data and has since been refined twice [2, 3]. The room-temperature structure of KSCN has an orthorhombic unit cell with the space-group symmetry, $Pbcm$, containing four potassium ($K+$) ions and four thiocyanate (SCN^-) ions. From figure 1 it can be seen that the potassium and thiocyanate ions occupy alternate layers perpendicular to the z axis in the unit cell.

The interest that has been shown in the alkali thiocyanates is due to their 'ball and rod' structures which consist of spherical, metal cations and linear, molecular anions. The vibrational modes arising from deformations of the thiocyanate molecules are known as internal modes and generally have frequencies higher than those for the external modes which involve only rigid-body translations of the ions.

The orthorhombic to tetragonal transition in KSCN, first discovered by Wrzewnewsky in 1912 [4] was later described by Klement [5] as predominantly higher-order with a small first-order component. Although the lack of hysteresis in the molar volume at T_c was typical of a higher-order transition, the small first-order component was necessary to account for the variation of T_c with pressure. Kinsho *et al* [6] later verified this when they discovered a small discontinuity in the enthalpy of the crystal at the transition.

In 1963, Sakiyama *et al* [7] suggested that the thiocyanate ions become disordered between two orientations obtained by a 180° end-for-end rotation during the transition. This was soon confirmed when single-crystal, x-ray data [8] showed that

0953-8984/92/397851+14$04.50

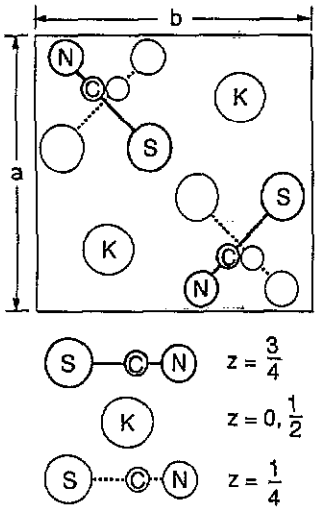

Figure 1. The KSCN unit cell.

the high-temperature phase had a tetragonal structure with the dipole moments of the thiocyanate ions disordered throughout the lattice. Three additional phase transitions for KSCN were later discovered using DTA measurements at pressures between atmospheric and 44 kbar [9]. These phase transitions were interpreted as marking further stages in the disordering of the SCN^- orientations. No phase transitions have been observed at temperatures below 340 K by either heat capacity [10] or DTA measurements [7].

Various authors have made Raman and infrared measurements of both the internal and external modes of KSCN [7, 11–14]. Certain optic modes have been studied at various temperatures [12, 15] and their behaviour related empirically to some simple models.

Although a number of the external phonon modes have been measured in KSCN at high temperatures [12] no single soft mode has been observed. Instead, several modes appear to decrease in energy as the temperature increases towards the transition temperature T_c. The optic mode at 122 cm^{-1} (3.66 THz) in KSCN has come under particular scrutiny [15] and its linewidth starts increasing with temperature at least 30 K below the transition. Of the internal modes, only the in-plane bending frequency, ν_{2a}, exhibits a temperature dependence [7]. This was attributed to a greater degree of coupling between the internal, in-plane, bending modes and the external librations of the SCN^- ions.

Our own measurements [16] are the only elastic and inelastic neutron scattering measurements of KSCN so far reported. The bulk of this investigation is concerned with the detailed presentation of ultrasonic sound velocity and thermal neutron scattering measurements of KSCN. In a subsequent paper a force constant model which has been developed in conjunction with this study will be presented.

2. Sample preparation

A number of large single crystals of KSCN were grown from aqueous solutions. The crystals had the approximate dimensions 50 mm × 50 mm × 5 mm with the x

direction along the shortest dimension. Neutron photographs and neutron rocking curves of these crystal samples confirmed that they contained no obvious twins. The extreme hygroscopicity of KSCN severely limited the time that the samples could be handled in the open. The crystals were very brittle and care had to be taken in their cutting and mounting.

For the room temperature, inelastic, neutron scattering measurements the crystal samples were glued to quartz glass supports with 'Five Minute Araldite' and sealed with a desiccant inside a quartz glass dome. The increase in the incoherent neutron scattering due to the quartz dome was negligible when studying the elastic peaks of the crystal. However, second-order scattering meant that for some of the inelastic measurements the scattering from the quartz could not be ignored.

The KSCN samples used for ultrasonic measurements were cut from the smaller crystals grown from aqueous solution. After checking for twins under crossed polarizers, the samples had to be cut so that two faces were parallel to within 10′ of arc and within 0.5° of a particular crystallographic direction. Each crystal piece was glued with Perspex dissolved in chloroform, on to a two-circle goniometer and aligned with the aid of Laue back-reflection photographs. The brass plate to which the sample was glued had an air-tight cover with a Mylar window which kept the crystal dry during the course of the alignment. Each exposure took 3.5 hours using a tungsten x-ray tube operating at 25 kV and 15 mA. Aligning the crystal along a symmetry direction was straightforward but determining this crystallographic direction was very difficult as the a and b lattice parameters are nearly equal. A Laue simulation program [17] was used to give the expected patterns for various directions. These simulations did not give all the correct intensities for the reflection spots, but aided in differentiating between the x and y directions.

After aligning the crystal, the goniometer was transferred to a grinding rig where a flat surface perpendicular to the aligned direction was ground on the crystal using 'wet and dry' paper down to 1200 grade. The crystal was then removed from the goniometer and the ground side stuck to the plunger of a polishing chase so that the opposite side could then be ground flat on 1200 grade paper. Finally, the faces of the sample were polished with 5 μm alumina grit moistened with n-butyl acetate just prior to mounting the crystal in the ultrasonic rig. The sensitivity of the sample surfaces to humidity meant that the final polishing had to be done in a glove bag under a dry nitrogen atmosphere.

3. Structural measurements

The values of the room temperature lattice parameters a and b, obtained in 1968 from single-crystal x-ray data, [3] were virtually swapped around from those measured ten years earlier by x-ray powder diffraction [18]. In order to resolve these discrepancies, a structure refinement was performed using neutron powder diffraction data.

About five grams of dried KSCN powder were loaded into a vanadium can in a dry nitrogen atmosphere and sealed against moisture using an indium metal gasket. The neutron diffraction data were collected at room temperature on the HRPD at the HIFAR reactor at the Lucas Heights Research Laboratories, Sydney. A modified Rietveld program [19] was then used to obtain the atomic positions and lattice parameters (table 1).

The atomic positions were in good agreement with those of Akers *et al* [3], the greatest difference being in the atomic positions of the carbon and nitrogen atoms

Table 1. Atomic positions and thermal parameters for KSCN. $a = 6.707(5)$ Å, $b = 6.691(5)$ Å, $c = 7.621(5)$ Å.

Atom	x	β_{11}	y	β_{22}	z	β_{33}	β_{12}
K	0.2080(8)	0.0183(14)	0.25	0.0122(14)	0	0.0071(7)	0
S	0.6050(9)	0.0100(13)	0.1087(9)	0.0107(13)	0.25	0.0102(11)	0.0008(8)
C	0.7704(4)	0.0083(5)	0.2871(3)	0.0091(4)	0.25	0.0103(5)	0.0014(4)
N	0.8890(3)	0.0116(4)	0.4154(3)	0.0126(4)	0.25	0.0180(5)	0.0039(4)

[20]. The neutron lattice parameters, however, were found to agree closely with the x-ray lattice parameters measured by the US Bureau of Standards [18]. The lattice parameters determined using elastic neutron diffraction were used for all subsequent neutron scattering experiments on KSCN.

4. Ultrasonic measurements

The ultrasonic sound velocities were measured using the same pulse-echo overlap technique [21] that Irving *et al* used for measuring sound velocities in CsSCN [22]. This technique measures time delays between successive echoes of a pulse of sound between parallel faces of the sample.

Crystal samples were prepared with faces parallel to the [100], [010] and [001] directions with thicknesses of between 4 mm and 6 mm. For transverse measurements, the alignment of the transducer polarization relative to the crystallographic directions was achieved by eye to an accuracy of $\pm 5°$. Any error in this alignment would not affect the measured velocity of a given mode but could introduce another echo train corresponding to the other transverse polarization mode. This was not observed, so the error due to this type of misalignment was assumed to be negligible.

The transducer mount and samples were enclosed by a glove bag filled with dry nitrogen to stop the sample faces being degraded in atmospheric moisture. In spite of this precaution, the polished faces of the samples suffered some degradation over the duration of the experiment.

For orthorhombic crystals there are nine independent elastic stiffness constants, c_{11}, c_{22}, c_{33}, c_{44}, c_{55}, c_{66}, c_{12}, c_{13} and c_{23}. From the velocity measurements taken in the [100], [010] and [001] directions, only the diagonal (c_{ii}) elastic constants could be calculated. Unfortunately there were not enough suitable crystal pieces to prepare samples with orientations in the [110], [101] and [011] directions. In order to gain a complete set of velocity measurements, the estimated initial slopes of the acoustic phonon branches measured by inelastic neutron scattering in the [110], [101] and [011] directions were used. From these initial slopes and the diagonal elastic constants the off-diagonal constants c_{12}, c_{13} and c_{23} were derived.

The measured velocities and calculated elastic constants are given in table 2. The errors for the diagonal elastic constants were calculated from a one-cycle mismatch error of ± 0.1 μs. The errors of the diagonal elastic constants combine with the relatively large errors for the initial slope velocity measurements to give very large errors for the off-diagonal elastic constants. In spite of this, it can be seen that the c_{ij} values calculated from the transverse and longitudinal initial slopes are consistent to within the given error. When two values for a particular elastic constant were

Table 2. Ultrasonic velocities and the elastic constants for KSCN.

	Velocity (km s^{-1})	Error (km s^{-1})		c_{ij} (GPa)	Error (GPa)	$\langle c_{ij} \rangle$ (GPa)	⟨Error⟩ (GPa)
ν_{xx}	3.76	0.11	c_{11}	26.7	1.5	—	—
ν_{yy}	3.81	0.09	c_{22}	27.4	1.3	—	—
ν_{zz}	3.35	0.14	c_{33}	21.1	1.8	—	—
ν_{yz}	2.09	0.05	c_{44}	8.2	0.4	8.1	0.3
ν_{zy}	2.05	0.04	c_{44}	7.9	0.3		
ν_{xz}	1.80	0.03	c_{55}	6.1	0.2	6.1	0.2
ν_{zx}	1.79	0.03	c_{55}	6.1	0.2		
ν_{xy}	3.02	0.08	c_{66}	17.2	0.9	17.4	1.1
ν_{yx}	3.05	0.11	c_{66}	17.6	1.3		
$\nu_{[110]L}$	4.71	0.15	c_{12}	20.6	10.7	12.8	7.9
$\nu_{[110]T}$	2.20	0.07	c_{12}	9.0	5.2		
$\nu_{[101]L}$	3.60	0.13	c_{13}	11.9	6.7	8.6	5.7
$\nu_{[101]T}$	2.13	0.06	c_{13}	6.3	4.6		
$\nu_{[011]L}$	3.49	0.13	c_{23}	4.1	6.4	4.3	5.4
$\nu_{[011]T}$	2.26	0.06	c_{23}	4.5	4.1		

obtained, a weighted average $\langle c_{ij} \rangle$ of the two was taken. The error of $\langle c_{ij} \rangle$ was taken to be the unweighted average of the two experimental errors.

5. Room temperature inelastic neutron scattering

Phonon energies of a single large crystal (50 mm × 40 mm × 5 mm) were measured using the triple-axis neutron spectrometer (TAS) at the Australian Nuclear Science and Technology Organisation's High Flux Reactor HIFAR at their Lucas Heights Research Laboratories. Phonons were measured as energy lost to the crystal with a constant final neutron energy of typically 8 THz.

The collimations used in measuring the acoustic modes were: 1.0°, 0.7°, 0.65° and 3°. To increase the neutron flux and thus reduce the counting time required to measure the higher energy optic modes, half the sample to analyser collimator was removed. This increased the angular acceptance of the analyser from 0.626° to 1.3° which did not affect the energy resolution, but did increase the number of elastically scattered neutrons 'leaking through' when $E' - E$ was less than about 0.8 THz.

Although the quartz glass mount and protective dome were found to contribute significantly to the incoherent elastic scattering, this was mainly a problem associated with measuring the low-energy acoustic phonons.

Although the TAS could measure energy transfers of up to 20 THz, the only optic phonon branches measured above 5 THz proved to be spurious peaks due to second-order scattering from the quartz dome. It was concluded that the phonon resonances measured at 14 THz with Raman and IR scattering [14] were too weak to be measured with neutron scattering.

The measured energy peak profiles were fitted with Gaussians on sloping backgrounds using a general-purpose fitting program on a VAX VMS/11 minicomputer. Generally, for a peak to be considered statistically significant, a minimum of five points of the peak had to be at least four standard deviations above the background. Two Gaussians were fitted to a profile only if both peaks were resolvable by eye.

In some cases the full width at half maximum (FWHM) of a fitted resonance peak was significantly larger than the value expected for a given energy transfer and wavevector based on the known resolution function for the instrument under identical conditions. For the flatter optical branches, abnormally large halfwidths could not be attributed to bad focusing of the resolution function but indicated the peak was a superposition of two or more phonon resonances. For each suspected multiple peak, half the difference between the observed and the expected FWHM was added to the calculated fitting error.

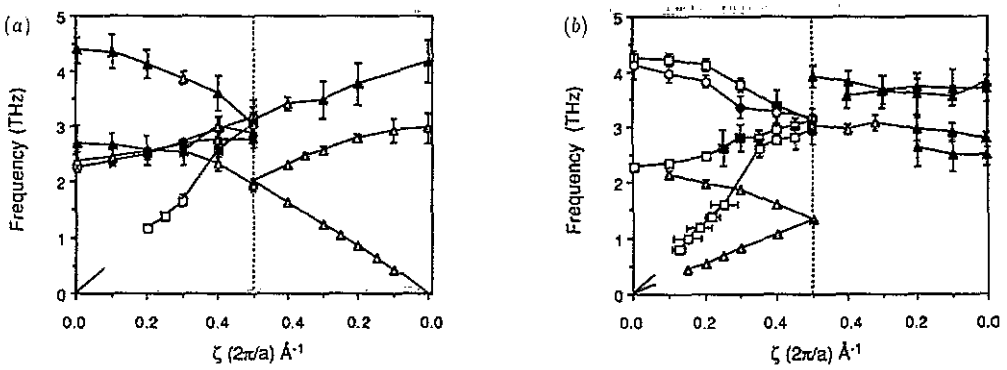

Figure 2. (*a*) KSCN phonons at room temperature, [ζ00] direction (*xy* plane), (□) L[100], (△) T[010], (○) unknown. (*b*) KSCN phonons at room temperature, [ζ00] direction (*xz* plane), (□) L[100], (△) T[001], (○) unknown.

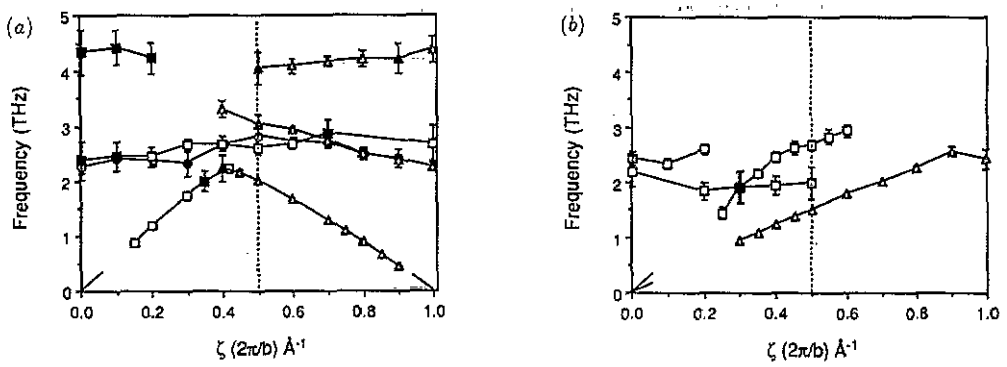

Figure 3. (*a*) KSCN phonons at room temperature, [0ζ0] direction (*yx* plane), (□) L[010], (△) T[100], (○) unknown. (*b*) KSCN phonons at room temperature, [0ζ0] direction (*yz* plane), (□) L[010], (△) T[001], (○) unknown.

All the measured phonon branches are shown in figures 2 to 7. The horizontal error bars in figure 2(*b*) indicate the peak fitting errors for the constant energy scans made on the [100] longitudinal acoustic branch, all the other phonons were measured at constant Q. The horizontal error bars for all but the phonons measured at constant energy were smaller than the plotted symbols. The solid symbols indicate suspected multiple peak resonances and their error bars are therefore generally larger. Data points without error bars had errors of less than ±0.04 THz. Although the peak fitting error was frequently less than ±0.01 THz, the minimum error for all

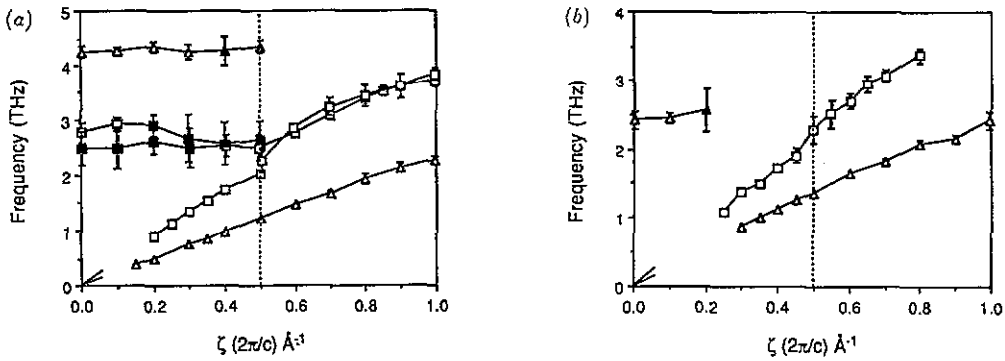

Figure 4. (*a*) KSCN phonons at room temperature, [00ζ] direction (zx plane), (□) L[001], (Δ) T[100], (○) unknown. (*b*) KSCN phonons at room temperature, [00ζ] direction (zy plane), (□) L[001], (Δ) T[010], (○) unknown.

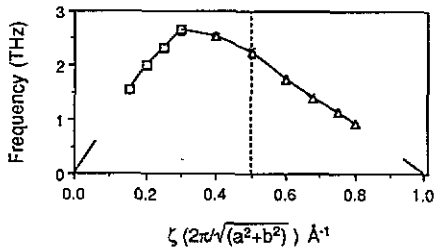

Figure 5. KSCN phonons at room temperature, [ζζ0] direction (xy plane), (□) L[110], (Δ) T[1 −1 0].

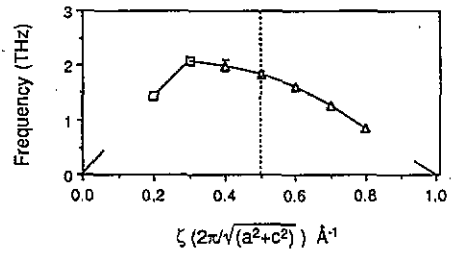

Figure 6. KSCN phonons at room temperature, [ζ0ζ] direction (xz plane), (□) L[101], (Δ) T[1 0 −1].

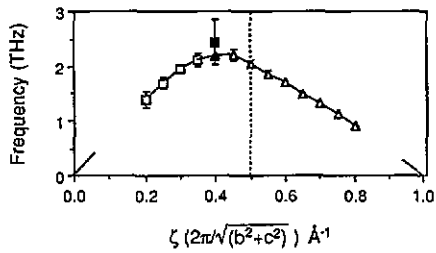

Figure 7. KSCN phonons at room temperature [0ζζ] direction (yz plane), (□) L[011], (Δ) T[0 1 −1].

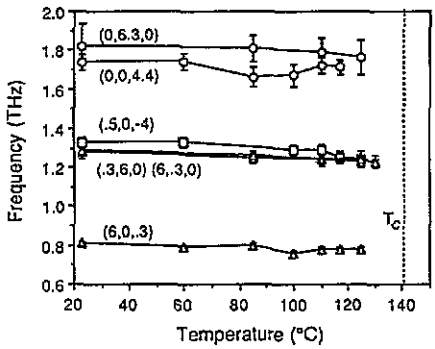

Figure 8. Acoustic mode frequencies at different temperatures.

measured energy transfers was taken to be ±0.03 THz due to possible calibration and alignment errors on the TAS.

The initial slopes of the acoustic branches as measured by ultrasonics are shown for the [100]-type directions in figures 2 to 4. As can be seen from these figures, there

was good agreement between the initial slopes determined from inelastic neutron scattering and from the ultrasonic velocities. The largest disagreement was in the longitudinal x direction where the acoustic phonon energies were hardest to measure due to their proximity to a strong elastic peak. For the [110], [101] and [011] directions, in which no ultrasonic velocities were measured, the initial slopes were estimated simply from the line drawn between the origin and the first phonon point.

The measured phonons were designated as longitudinal or transverse depending on whether the resonance was measured with the scattering vector Q roughly parallel or perpendicular to the phonon wavevector q. Phonons labelled as unknown were measured at places in reciprocal space where the Q and q vectors were neither parallel nor perpendicular. The solid lines connect phonons measured with similar scattering vectors but do not necessarily connect phonons belonging to the same branch.

Phonons measured along all but the [100] directions are plotted on an extended zone to highlight the fact that they are doubly degenerate at the Brillouin zone boundary as predicted by group theory. An analysis of the symmetry of KSCN has indicated that all the branches in the [100] direction are singly degenerate at the zone boundary [23]. It should be noted that for clarity in figures 2(a) and (b) the branches in the [100] direction have been split into two groups even though the zone is not extended.

Unfortunately, although phonons measured at similar scattering vectors often belonged to the same branch, not every branch could be followed all the way from the zone centre to the zone edge. The relatively large number of vibrational modes meant that many phonon eigenvectors tended to 'mix' which caused some branch resonances to fade in intensity or jump discontinuously in energy as they were followed out from the zone centre. A typical example of this was the longitudinal acoustic mode in figure 2(b) which was measured in reciprocal space at $(6\zeta, 0, 0)$. At $\zeta = 0.3$ the inelastic scattering intensity for another mode with higher energy became significant, making the total resonance peak very broad. At $\zeta = 0.45$ the scattering intensity for the original branch had almost completely faded leaving a narrower peak centred on the higher branch.

To maximize the chances of finding phonons with the limited amount of beam time available, a uniaxial inter-atomic force constant model [23] was used to calculate likely vibrational modes and hence dynamical structure factors for the phonon branches at different points in reciprocal space. These facilitated the choice of suitable scattering vectors at which to look for unmeasured modes and aided in identifying the symmetries of the measured modes.

6. High-temperature measurements of KSCN

A number of phonon modes were believed to be librational in nature on the basis of model calculations performed for the KSCN structure [23]. It was therefore considered worthwhile to measure the frequencies of these modes at temperatures approaching T_c.

A furnace was constructed such that a large single crystal could be sandwiched between two thin aluminium plates which were in good thermal contact with heating blocks above and below the sample. The clamped crystal was sealed with desiccant within a quartz glass tube. The temperature of the crystal was maintained with a stability of better than ± 0.5 °C and varied by no more than 1 °C over the entire crystal.

The shifts in the lattice parameters relative to their room temperature (23 °C) values were determined by using the TAS set up for elastic scattering to measure the Bragg angles for pairs of reflections along each of the principal directions in reciprocal space. The pairs of reflections used were: (300) and (600), (040) and (060), and (004) and (006) for the x, y, and z directions respectively. The lattice parameters measured at different temperatures using the TAS are shown in table 3.

Table 3. Lattice parameters for KSCN at higher temperatures.

Temperature (°C)	a (Å)	b (Å)	c (Å)
23	6.707(5)	6.691(5)	7.621(5)
60	6.710(12)	—	7.648(13)
85	6.719(12)	6.704(12)	7.676(13)
100	6.726(12)	—	7.707(13)
110	6.726(12)	6.700(12)	7.711(13)
125	6.728(12)	6.707(12)	7.753(13)

The large single-crystal KSCN samples used in the furnace were not as good in quality as the sample used in the room temperature measurements. Although these crystals were single and larger than the first sample, they had smaller coherent elastic and inelastic scattering peaks. This was attributed to a higher content of water trapped as small inclusions of saturated solution inside the samples. If no previous high-temperature measurements had been made on a sample, the coherent elastic scattering was found to improve if the new crystal was held at 110 °C in the furnace under a vacuum for about six hours.

The increase of incoherent scattering with temperature and the inferior quality of the single-crystal samples used in the furnace meant that longer counting times were required to achieve the same peak-to-background ratio as those measured during the room temperature phonon measurements. Selected phonon resonances were measured at different temperatures and with limited statistics.

19 phonon resonances were measured at temperatures ranging from 23 °C (room temperature) to 110 °C, a subset of this total was measured at higher temperatures to a maximum of 130 °C. Of the 19 resonances, 6 belonged to acoustic branches which were believed to have insignificant amounts of libration of the SCN^- ions. The main reason for measuring these acoustic modes was to ensure that the angle calibrations and lattice parameters were correct for each run of phonon measurements at a particular temperature. As the acoustic branches were generally the steepest, they were expected to show the greatest sensitivity to any angular misalignment of the sample or error in the lattice parameters.

The measured acoustic phonon energies (figure 8) showed a gradual decrease in energy with increasing temperature. With the exception of the longitudinal phonon at $Q = (0,0,4.4)$, the FWHMs of the acoustic phonon resonances were constant to within ± 0.04 THz for all temperatures. A small apparent increase in energy (0.04 THz) for the $(0,0,4.4)$ phonon energy above 100 °C was probably an artifact of the fitting procedure. The measured integrated intensities of the acoustic phonons showed a general decrease with increasing temperature, again with the exception of the $(0,0,4.4)$ phonon.

In contrast to the acoustic phonons, the optic phonons show marked variations in energy, width and integrated intensity at different temperatures (figure 9). This

was attributed to the fact that many of the measured optic phonons were likely to be superpositions of two or more resonances. At different temperatures, the relative structure factors of all the modes contributing to a given energy profile could change. This would have the effect of altering the position, width and intensity of the measured peak, even if the widths and positions of the constituent resonances were unchanged.

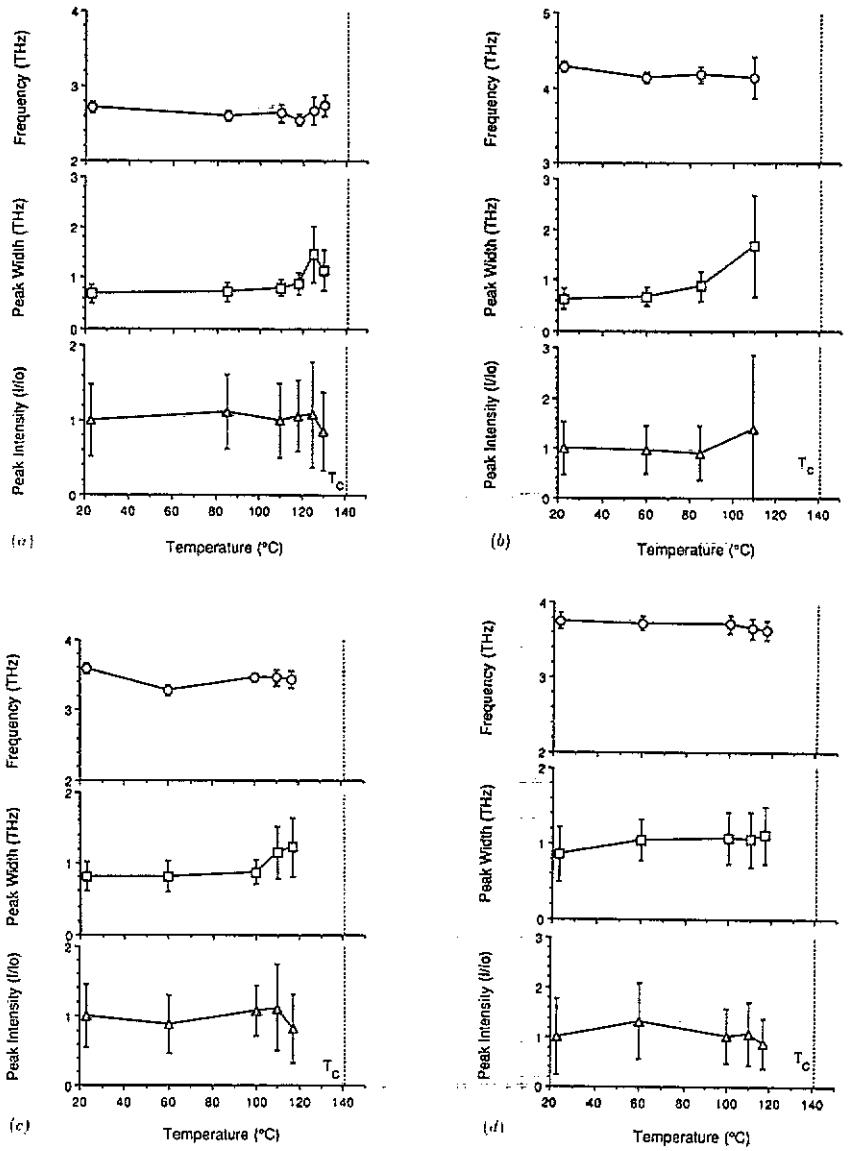

Figure 9. Temperature behaviour of optic phonon resonance at (*a*) $Q = (-3.3, 5, 0)$, (*b*) $Q = (7, 0, 0)$, (*c*) $Q = (0, 0, 4.9)$, (*d*) $Q = (0.1, 0, -5)$.

Figure 9 shows the energies, widths and integrated intensities of four of the 13 optic modes measured at different temperatures. The modes measured at $Q = (-3.3, 5, 0)$ and $(7, 0, 0)$ in figures 9(*a*) and (*b*) were singled out because they

exhibited variations in the peak parameters that became more rapid as T approached T_c, possibly as a precursor to the transition. It is likely that the apparent decrease in the width of the $(-3.3,5,0)$ resonance near T_c is due to interpretational problems associated with fitting the measured profile. The modes measured at $Q = (0,0,4.9)$ and $(0.1,0,-5)$ in figures 9(*c*) and (*d*) had frequencies near the 3.66 THz Raman mode investigated by Owens *et al.* Although these measured profiles could not be characterized mathematically, they did show qualitative trends similar to those found for the 3.66 THz Raman mode in that their peak widths increased and frequencies softened as $T \rightarrow T_c$.

7. Discussion

The room temperature structure of CsSCN is similar to that for KSCN in that the thiocyanate ions are constrained to librate in the mirror plane layers [24].

Table 4. Comparison of elastic properties of KSCN and CsSCN.

c_{ij}	KSCN (GPa)	CsSCN (GPa)		KSCN	CsSCN
c_{11}	26.7	18.9	Bulk modulus (GPa)	13.3	13.2
c_{22}	27.4	20.6			
c_{33}	21.1	28.1	Linear compressibility		
c_{44}	8.1	2.0	(GPa^{-1})		
c_{55}	6.1	7.3	along [100]	0.014	0.029
c_{66}	17.4	3.0	along [010]	0.024	0.034
c_{12}	12.8	7.7	along [001]	0.037	0.012
c_{13}	8.6	6.2			
c_{23}	4.3	14.9			

In table 4, the elastic parameters for KSCN derived from the ultrasonic measurements are compared with those for CsSCN [22]. In general, the linear compressibilities for both structures are greatest perpendicular to the mirror planes (the z direction for KSCN and the y direction for CsSCN). The shear elastic constants for KSCN are larger than those for CsSCN with the largest constants in both crystals relating to shear strains lying parallel to the mirror planes (c_{66} in the xy plane for KSCN and c_{55} in the xz plane for CsSCN). The elastic constants of both structures give rise to very similar values for the bulk moduli.

The elastic Debye temperature (θ_D^{el}) for CsSCN is 132 K [22]. The ratio of the θ_D^{el} values for KSCN and CsSCN was found to obey the relation

$$\theta_D^{el}(\mathrm{KSCN})/\theta_D^{el}(\mathrm{CsSCN}) = (M_{\mathrm{CsSCN}}/M_{\mathrm{KSCN}})^{1/3}$$

where M_{KSCN} and M_{CsSCN} are the masses of the molecular units. This indicated that the difference in θ_D^{el} was mainly due to the difference in the molecular masses.

In table 5 the zone-centre phonons measured on the TAS are compared with Raman and infrared frequencies collected from the literature [25]. The energy resolution of the TAS was probably not sufficient to resolve a number of the phonons, especially

Table 5. KSCN external mode frequencies as measured by inelastic neutron scattering and Raman spectroscopy.

TAS measurements			Raman and IR measurements					
Q	Frequency (THz)	Error (THz)	Frequency (THz)					
(0, 1, 6)	2.20	0.28	1.97	2.04	2.04			
(3, 5, 0)	2.25	0.08						
(6, 0, 1)	2.27	0.06						
(1, 7, 0)	2.37	0.16	2.34					
(0, 6, 1)	2.41	0.12						
(0, 1, 4)	2.43	0.18						
(1, 0, 5)	2.50	0.31						
(2, 7, 0)	2.69	0.33						
(1, 0, 6)	2.77	0.18	2.88	2.88				
(1, 6, 0)	2.97	0.28	2.94	3.05	3.12	3.36	3.36	3.44
(0, 0, 5)	3.70	0.10	3.66	3.66	3.69	3.72		
(0, 0, 7)	3.83	0.11	3.78					
(7, 0, 3)	4.13	0.26	4.13					
(0, 7, 0)	4.18	0.37	4.28					
(7, 0, 0)	4.25	0.11	4.32	4.35				
			4.58	4.80				

in the 2.7–3.7 THz range. In addition to this, some of the zone-centre phonons measured on the TAS in the range 2.2–2.6 THz do not seem to correspond to any Raman or infrared frequencies. Although some of the peak resonances measured on the TAS may belong to the same phonon mode, there are still six unmeasured infrared-active optic modes below 5 THz that may account for the gaps in table 5.

According to Ti *et al* [14], of the 48 phonon branches, four lie at about 60 THz, 4 at 22 THz, 8 at 14 THz with the remaining 32 modes appearing below 5 THz. Although more than 40 branches below 5 THz have been at least partly measured, many branches, like the longitudinal acoustic ones, have been measured twice in different planes.

A better understanding of the inter-atomic potentials will undoubtedly be obtained by comparing the high-temperature phonon dispersion behaviour of KSCN with that for an isomorphic structure. In figure 10 the lattice parameters of KSCN measured on the TAS are compared with the high-temperature lattice parameters for RbSCN [9] measured by x-ray diffraction. Taking the different transformation temperatures into account, there seems to be a qualitative similarity in the temperature dependences of the lattice parameters for the two structures.

Rietveld analysis of neutron powder diffraction data of RbSCN would be an ideal way to confirm Klement's conclusion [5] that KSCN and RbSCN are isomorphic both above and below their respective phase transition temperatures. If the structures are isomorphous, RbSCN will be the logical crystal to study in further investigations aimed at comparing the lattice dynamical behaviour of the alkali metal thiocyanates.

8. Conclusion

The elastic behaviour of KSCN was found to resemble that of CsSCN at room temperature, with the bulk moduli and elastic Debye temperatures showing similar values

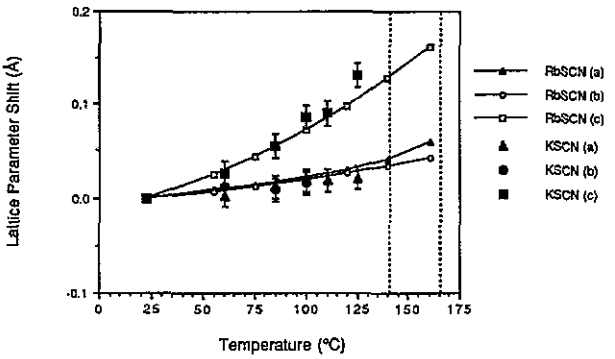

Figure 10. Shift in lattice parameters with increasing temperature: KSCN (solid data points) and RbSCN (solid line).

(table 2). The most obvious similarity between the two crystals was that both exhibited the greatest shear stiffness in the plane parallel to their mirror planes (the xy plane for KSCN and xz plane for CsSCN). The phase velocities were generally higher for acoustic waves involving atomic displacements parallel to these planes. From this it was concluded that, on average, the atomic bonds lying parallel to the mirror planes in both KSCN and CsSCN were stronger than those lying perpendicular to these planes.

A large number of phonon groups was measured below 5 THz for KSCN and the detected frequencies appeared to be in broad agreement with previously measured Raman and infrared data in this range (table 5). Phonons with frequencies in the 14 THz range were not detected on the TAS, probably on account of the small scattering cross sections for the modes.

The acoustic phonon frequencies for KSCN measured at temperatures up to 125 °C (16 °C below the transition temperature) were all found to soften gradually with increasing temperature. This was very similar to the behaviour of the acoustic modes in CsSCN reported by Irving *et al* [26].

With increasing temperatures, the measured optic-mode frequencies showed fluctuations in energy and halfwidth far greater than those for the acoustic frequencies. This can be attributed in part to the softening of some of the librational lattice modes as the transition temperature is approached, but is more probably due to the scattering cross sections of various superimposed optic modes changing relative to each other with increasing temperature.

A Rietveld analysis of neutron diffraction data from a powder sample of RbSCN could confirm Klement's conclusion [5] that RbSCN and KSCN are isomorphous. If RbSCN is found to be isomorphous with KSCN, a comparison of the lattice dynamics of the two crystals will be particularly illuminating. This, in addition to further inelastic neutron studies of both CsSCN and KSCN at temperatures nearer, and even above their transition temperatures, should enhance our understanding of the lattice dynamics of the alkali thiocyanates gained through the present work.

Acknowledgments

The financial support of the Australian Institute of Nuclear Science and Engineering and the Australian Research Grants Scheme is acknowledged. One of us (DJC) is most grateful for the award of a studentship by the Australian Institute of Nuclear

Science and Engineering. We also acknowledge the availability of the facilities at the Australian Nuclear Science and Technology Organisation.

References

[1] Klug H P 1933 *Z. Kristallogr.* **85** 214–22
[2] Bussem W R, Gunther P and Tubin R Z 1934 *Phys. Chem.* B **24** 1
[3] Akers C, Peterson S W and Willet R D 1968 *Acta Crystallogr.* B **24** 1125–6
[4] Wrzewnewsky J B 1912 *Z. Anorg. Chem.* **74** 95
[5] Klement W Jr 1976 *Bull. Chem. Soc. Japan* **49** 2148–53
[6] Kinsho Y, Onodera N, Sakiyama M and Seki S 1979 *Bull. Chem. Soc. Japan* **52** 395–402
[7] Sakiyama M, Suga H and Seki S 1963 *Bull. Chem. Soc. Japan* **36** 1025–31
[8] Yamada Y and Watanabe T 1963 *Bull. Chem. Soc. Japan* **36** 1032–7
[9] Pistorius C W F T, Clark J B and Rapoport E J 1968 *Chem. Phys.* **48** 5123–31
[10] Vanderzee C E and Westrum E F 1970 *J. Chem. Thermodyn.* **2** 417–29
[11] Jones L H 1958 *J. Chem. Phys.* **28** 1234–6
[12] Iqbal Z, Sharma L H and Moller K D 1972 *J. Chem. Phys.* **57** 4728–37
[13] Dao N G and Wilkinson G R 1973 *J. Chem. Phys.* **59** 1319–24
[14] Ti S S, Kettle S F A and Ra O 1976 *Spectrochimica Acta* A **32** 1603–13
[15] Owens F J 1979 *Solid State Commun.* **29** 789–91
[16] Cookson D J, Elcombe M M and Finlayson T R 1987 *Solid State Commun.* **3** 357–9
[17] Cornelius C A 1981 *Acta Crystallogr.* A **37** 430–6
[18] *US NBS Circular 539* 1958 vol 8, pp 44–5
[19] Hill R J and Howard C J 1985 *J. Appl. Crystallogr.* **18** 173–80
[20] Cookson D J, Elcombe M M and Finlayson T R 1988 *Mater. Sci. Forum* **27/28** 113–6
[21] Papadakis E 1967 *J. Acoust. Soc. Am.* **42** 1045–51
[22] Irving M A, Prawer S, Smith T F and Finlayson T R 1983 *Aust. J. Phys.* **36** 85–92
[23] Cookson D J, Elcombe M M and Finlayson T R 1992 Theoretical modelling of phonon dispersion relations in alkali thiocyanates *J. Phys.: Condens. Matter* to be submitted
[24] Manolatos S, Tillinger M and Post B 1973 *J. Solid State Chem.* **7** 31–5
[25] Ti S S and Ra O 1980 *J. Chem. Phys.* **73** 5738–48
[26] Irving M A, Elcombe M M and Smith T F 1985 *Aust. J. Phys.* **38** 85–95